The EMBO Journal (2008) 27, 692–703 | © 2008 European Molecular Biology Organization | All Rights Reserved 0261-4189/08
www.embojournal.org

THE EMBO JOURNAL

Cardiac pacemaker function of HCN4 channels in mice is confined to embryonic development and requires cyclic AMP

Dagmar Harzheim[1,6], K Holger Pfeiffer[1], Larissa Fabritz[2], Elisabeth Kremmer[3], Thorsten Buch[4], Ari Waisman[5], Paulus Kirchhof[2], U Benjamin Kaupp[1,7,*] and Reinhard Seifert[1,*]

[1]Forschungszentrum Jülich, Institut für Neurowissenschaften und Biophysik, Abteilung Zelluläre Biophysik, Jülich, Germany, [2]Medizinische Klinik und Poliklinik C, Universitätsklinikum Münster und IZKF Münster, Münster, Germany, [3]GSF, Institut für Molekulare Immunologie, München, Germany, [4]Institut für Experimentelle Immunologie, Universität Zürich, Zürich, Switzerland and [5]I Medizinische und Poliklinik, Johannes Gutenberg-Universität Mainz, Mainz, Germany

Important targets for cAMP signalling in the heart are hyperpolarization-activated and cyclic nucleotide-gated (HCN) channels that underlie the depolarizing 'pacemaker' current, I_f. We studied the role of I_f in mice, in which binding of cAMP to HCN4 channels was abolished by a single amino-acid exchange (R669Q). Homozygous $HCN4^{R669Q/R669Q}$ mice die during embryonic development. Prior to E12, homozygous and heterozygous embryos display reduced heart rates and show no or attenuated responses to catecholaminergic stimulation. Adult heterozygous mice display normal heart rates at rest and during exercise. However, following β-adrenergic stimulation, hearts exhibit pauses and sino-atrial node block. Our results demonstrate that in the embryo, HCN4 is a true cardiac pacemaker and elevation of HCN4 channel activity by cAMP is essential for viability. In adult mice, an important function of HCN4 channels is to prevent sinus pauses during and after stress while their role as a pacemaker of the murine heart is put into question. Most importantly, our results indicate that HCN4 channels can fulfil their physiological function only when cAMP is bound.

The EMBO Journal (2008) **27,** 692–703. doi:10.1038/emboj.2008.3; Published online 24 January 2008
Subject Categories: development; molecular biology of disease
Keywords: cardiology; cyclic nucleotides; heart; ion channel; signalling

*Corresponding authors. UB Kaupp and R Seifert, Institut fuer Neurowissenschaften, Forschungszentrum Juelich, INB-1, Jülich 52425, Germany. Tel.: +49 2461 6140 41; Fax: +49 2461 6142 16;
E-mail: a.eckert@fz-juelich.de, r.seifert@fz-juelich.de
[6]Present address: Laboratory of Molecular Signalling, The Babraham Institute, Babraham Research Campus, Cambridge CB22 3AT, UK
[7]Present address: Stiftung Caesar, Ludwig-Erhard-Allee 2, 53175 Bonn

Received: 22 March 2007; accepted: 21 December 2007; published online: 24 January 2008

Introduction

Spontaneous activity of the mammalian heart is generated in the sino-atrial node (SAN). How pacemaker activity is generated in SAN cells and how pacemaking is regulated by the autonomous nervous system is still a matter of debate. A number of different ion channels and signalling events have been implicated in pacemaker activity (for review see, Couette *et al*, 2006). Key players controlling the diastolic depolarization are the hyperpolarization-activated current I_f and the L-type calcium current $I_{Ca,L}$ (DiFrancesco, 1993; Verheijck *et al*, 1999; Biel *et al*, 2002; Zhang *et al*, 2002; Mangoni *et al*, 2003; Barbuti *et al*, 2007).

The I_f current is mediated by hyperpolarization-activated and cyclic nucleotide-gated (HCN) channels. These channels have a number of particular features that enable them to open at voltages near the maximal diastolic potential (MDP). First, channels are activated on hyperpolarization of the membrane potential. Second, channel activity is dependent on the intracellular cAMP concentration ($[cAMP]_i$) (DiFrancesco and Tortora, 1991). When cAMP binds to the cyclic nucleotide-binding domain (CNBD) of HCN channels, the activation curve shifts towards more positive voltages, thereby enhancing channel activity. In addition, channels with cAMP bound activate faster and deactivate slower. Thus, an increase of $[cAMP]_i$, for example, during β-adrenergic stimulation, enhances I_f, whereas a decrease of $[cAMP]_i$, for example, during muscarinic stimulation, attenuates I_f (DiFrancesco *et al*, 1986; DiFrancesco and Tromba, 1988). It has been proposed that cAMP modulation of I_f is the primary pathway by which the autonomous nervous system controls the heart rate (Bucchi *et al*, 2003). Consistent with this model, mutations in the HCN4 channel gene, the major isoform in the SAN, are associated with sinus bradycardia and arrhythmia (Schulze-Bahr *et al*, 2003; Milanesi *et al*, 2006).

The other key player in cardiac pacemaking is the voltage-dependent Ca^{2+} channel $Ca_v1.3$ that carries $I_{Ca,L}$. The $I_{Ca,L}$ is activated during the early phase of the diastolic depolarization, and inhibition of $I_{Ca,L}$ induces bradycardia *in vivo* (Lande *et al*, 2001). Moreover, $Ca_v1.3$ knockout mice are bradycardic and show sino-atrial arrhythmia (Platzer *et al*, 2000; Zhang *et al*, 2002; Mangoni *et al*, 2003). These observations have led to the proposal that in SAN cells $Ca_v1.3$ channels generate a significant electrical signal contributing to the diastolic depolarization (Couette *et al*, 2006). Within the framework of this model, the increase of $I_{Ca,L}$ during cAMP stimulation enhances the pacing component.

In addition to I_f and $I_{Ca,L}$, at least three other ionic pathways contribute to the regulation of the heart rate. One pathway is $I_{Ca,T}$, which is almost exclusively mediated by $Ca_v3.1$ channels (Mangoni *et al*, 2006). $Ca_v3.1$ knockout mice exhibit pronounced bradycardia and a significant slowing of atrioventricular (AV) conduction (Mangoni *et al*, 2006). Another current implied in pacemaker generation is a

sustained inward current, I_{st}, which was identified in spontaneously beating SAN cells (Guo *et al*, 1995). Its proposed role in cardiac pacemaking is largely based on numerical simulations of pacemaker activity (Shinagawa *et al*, 2000; Zhang *et al*, 2002). The impact of I_{st} on pacing the heart is difficult to estimate due to its unidentified molecular nature and the lack of specific pharmacological tools to target this current. Finally, rhythmic Ca^{2+} oscillations have been proposed to be involved in cardiac pacemaking. This proposal challenges the major role of I_f in primary pacemaker activity of the SAN and its role in the autonomous regulation of the heartbeat (Bogdanov *et al*, 2001; Kodama *et al*, 2002; Lipsius and Bers, 2003). Instead of I_f, electrogenic Na^+/Ca^{2+} exchange has been proposed to provide the major depolarizing pacemaking current. According to this model, SAN cells generate rhythmic, submembrane Ca^{2+} oscillations via spontaneous opening of ryanodine receptors in the sarcoplasmatic reticulum (SR) (Bogdanov *et al*, 2001). Thereby, the intracellular Ca^{2+} concentration is locally increased and the Na^+/Ca^{2+} exchanger in the plasma membrane is activated. An inward current is generated that depolarizes the cell. The frequency of spontaneous Ca^{2+} release events is tightly controlled by the efficiency of Ca^{2+} uptake into the SR by the Ca^{2+} ATPase SERCA. The pumping rate of SERCA is highly sensitive to changes in $[cAMP]_i$. An increase of $[cAMP]_i$ stimulates SERCA activity (for review see, Colyer, 1998; Kamp and Hell, 2000), leading to a higher SR Ca^{2+} uptake and spontaneous Ca^{2+} events occur more frequently. The heart beats faster.

Here, we investigate the role of HCN4 in cardiac pacemaking of mice using a knock-in mouse model in which cAMP binding to the HCN4 channel has been abolished. Our results are both intriguing and unexpected. They demonstrate that (1) in the embryo, HCN4 is a powerful pacemaker but only when cAMP is bound and (2) in adult mice, HCN4 does not seem to contribute to cardiac pacemaking, but rather ensures stable heart rhythm during and after stress.

Results

Generation of HCN4^{R669Q} knock-in mice

To define the physiological function of I_f and its modulation by cAMP more precisely, we generated knock-in mice that harbour a single amino-acid exchange (R669Q) in the CNBD of the HCN4 channel. This arginine residue is crucial for the binding of cAMP because it interacts with the negatively charged phosphate group (McKay *et al*, 1982; Bubis *et al*, 1988; Zagotta *et al*, 2003). To ascertain that the mutation abolishes regulation by cAMP, we analysed the wild-type HCN4 and the mutant HCN4^{R669Q} channel in Flp-In-293 cells. In the absence of cAMP, the voltage-dependent activation of HCN4^{R669Q} mutant and wild-type channels was similar (Figure 1A). Voltages of half-maximal activation $V_{1/2}$ were -94.3 ± 3.7 mV ($n=8$) for wild-type and -99.5 ± 3.4 mV ($n=7$) for HCN4^{R669Q} channels. Cyclic AMP shifted the activation curve of the wild-type HCN4 channel by $+24$ mV ($V_{1/2}=-70.6\pm2.7$ mV ($n=3$)), whereas no shift was observed for the HCN4^{R669Q} mutant ($V_{1/2}=-96.3\pm7.1$ mV ($n=5$)). We introduced the mutation into the HCN4 gene locus of mice via homologous recombination in embryonic stem cells (Figure 1B). Integration of the targeting vector, germ-line transmission, and deletion of the neomycin resistance gene were confirmed by Southern blot and PCR analysis (Figure 1C and D, and data not shown). Heterozygous HCN4$^{+/R669Q}$ mice were viable, bred normally, and were indistinguishable from wild-type littermates. However, no homozygous HCN4$^{R669Q/R669Q}$ pups were born from heterozygous matings (HCN4$^{+/+}$: 57/155; HCN4$^{+/R669Q}$: 98/155). Analysis of timed matings revealed that HCN4$^{R669Q/R669Q}$ embryos developed normally until E11, but were dead from E12 on (Figure 1E), indicating that homozygous embryos die between E11 and E12.

The amino-acid exchange R669Q does not alter protein expression of HCN4

We were concerned about the similar lethal phenotype of HCN4$^{-/-}$ (Stieber *et al*, 2003) and HCN4$^{R669Q/R669Q}$ mice. To investigate whether the pattern or level of expression of the channel mutant is altered, we analysed the cellular HCN4 distribution during embryonic development prior to E11.5. Different HCN4-specific antibodies labelled the same region in the heart of HCN4$^{+/+}$ and HCN4$^{R669Q/R669Q}$ embryos (Figure 2A). No obvious difference existed in the cellular distribution of the HCN4 channel in wild type compared to the HCN4^{R669Q} channel in homozygous embryos (Figure 2A, middle panel). A monoclonal, HCN4-specific antibody (specificity of HCN4 antibodies shown in Figure 2C) labelled two bands in western blots of membrane proteins from Flp-In-293 cells that expressed the HCN4 or the HCN4^{R669Q} channel (Figure 2B). Treatment with PNGase F revealed that the upper band represents a glycosylated form of the HCN4 channel. In western blots of proteins isolated from wild-type, heterozygous, and homozygous embryonic hearts, the antibody recognized the same protein bands with equal intensities, demonstrating that the mutation does not affect the level of HCN4 expression (Figure 2D).

HCN4$^{R669Q/R669Q}$ embryonic mice display reduced basal heart rates

We analysed the spontaneous beat frequency of hearts isolated from HCN4$^{+/+}$, HCN4$^{+/R669Q}$, and HCN4$^{R669Q/R669Q}$ embryos prior to E11.5. Under basal conditions, hearts from heterozygous and homozygous embryos beat regularly without obvious arrhythmias; however, the heart rate was significantly slower compared to hearts from wild-type embryos (Figure 2E and Table I). Furthermore, in wild-type embryos, the heart rate increased from E9 to E11 (Figure 2E and Table I), thereby enhancing supply of nutrients and oxygen necessary for proper development. This increase was not observed in HCN4$^{+/R669Q}$ embryos, and in HCN4$^{R669Q/R669Q}$ embryos, the heart rate was even further reduced from day 9.5 to 11.5 (Figure 2E). Notably, heart rates from HCN4$^{R669Q/R669Q}$ and HCN4$^{-/-}$ embryos at E9.5 (Stieber *et al*, 2003) are virtually identical, indicating that the Arg669Gln exchange completely eliminates the pacing function of the HCN4 channel.

Adrenergic stimulation does not accelerate the heart rate of HCN4$^{R669Q/R669Q}$ embryonic mice

Isoproterenol superfusion increased the rate of isolated hearts from HCN4$^{+/+}$ and HCN4$^{+/R669Q}$ embryos ($37.4\pm4.5\%$ ($n=8$) and $19.8\pm2.8\%$ ($n=6$), respectively), whereas no increase was observed in hearts from HCN4$^{R669Q/R669Q}$ embryos ($2.8\pm2.5\%$ ($n=5$); Figure 2F and G). Similarly,

superfusion with NKH477, a drug that specifically activates adenylyl cyclases, increased the heart rate from $HCN4^{+/+}$ and $HCN4^{+/R669Q}$ embryos (22.6±1.7% ($n=14$) and 14.2±2.6% ($n=13$), respectively), but not from $HCN4^{R669Q/R669Q}$ embryos (1.9±1.9% ($n=5$); Figure 2H and I). These results demonstrate that HCN4 is the principal target for cAMP during the embryonic stages analysed in this study. An acceleration of heartbeat frequency during β-adrenergic stimulation is only possible when cAMP binds to HCN4.

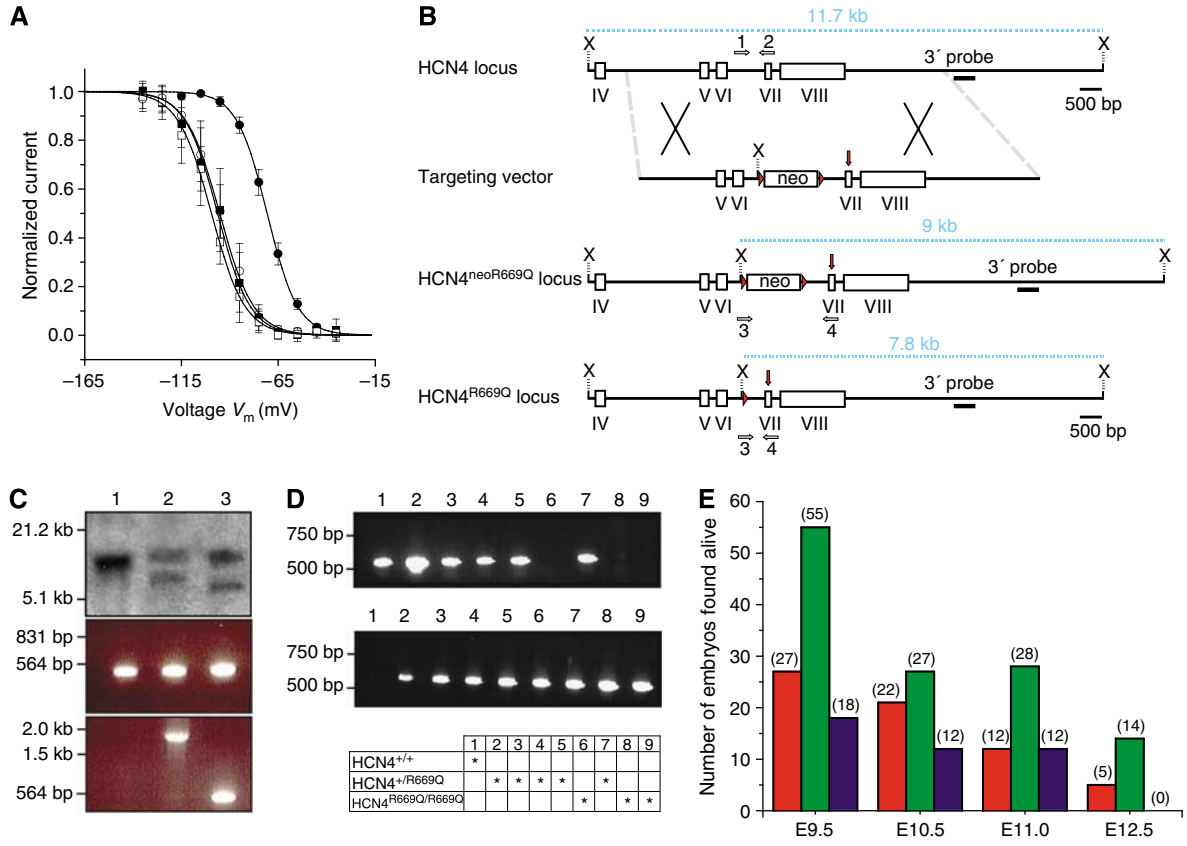

Figure 1 Embryonic death of $HCN4^{R669Q/R669Q}$ mice. (**A**) Voltage-dependent activation of heterologously expressed HCN4 (circles) and $HCN4^{R669Q}$ channels (squares). Voltages of half-maximal activation (±s.d.) in the absence (open symbols) and presence (filled symbols) of cAMP (100 μM) were −94.3±3.7 ($n=8$) and −70.6±2.7 mV ($n=3$) for HCN4, and −99.5±3.4 ($n=7$) and −96.3±7.1 mV ($n=5$) for $HCN4^{R669Q}$, respectively. (**B**) Targeting strategy. Only exons IV–VIII of the HCN4 locus are shown (white boxes). The targeting vector carried the mutation in exon VII (red arrow) and the neomycin resistance gene (neo), flanked by two loxP elements (red arrowheads). neo was deleted by Cre-mediated recombination. Homologous recombination and deletion of neo were detected through Southern blot using the *Xba*I restriction sites (X) and the 3′ probe (black box), and through PCR (primers 3 and 4, grey arrows). *Xba*I fragments that are recognized by the 3′ probe are depicted in blue. (**C**) Southern blot and PCR analysis of genomic DNA from $HCN4^{+/+}$ (lane 1), $HCN4^{+/neoR669Q}$ (lane 2), and $HCN4^{+/R669Q}$ (lane 3) mice. Upper panel: Southern hybridization of *Xba*I-digested DNA with the ^{32}P-radiolabelled 3′ probe. Middle panel: amplification of the wild-type allele (primers 1 and 2, 586 bp). Lower panel: amplification of the recombinant allele (primers 3 and 4, 1804 or 610 bp). (**D**) Genotyping of embryos from one litter. Upper panel: PCR amplifying the wild-type allele (primers 1 and 2). Middle panel: PCR amplifying the recombinant allele (primers 3 and 4). Lower panel: genotypes of analysed litter. (**E**) Number of embryos found alive (E9.5–E12.5; red: $HCN4^{+/+}$; green: $HCN4^{+/R669Q}$; blue: $HCN4^{R669Q/R669Q}$).

Figure 2 The $HCN4^{R669Q}$ channel alters the embryonic heartbeat. (**A**) Upper panels: cryo-sections from $HCN4^{+/+}$ (left) and $HCN4^{R669Q/R669Q}$ embryos (right) stained with an HCN4-specific antibody (PPc73K; bar: 100 μm). Middle panels: higher magnification of the labelled region (bar: 20 μm). Lower panels: Two independent HCN4-specific antibodies label identical structures in the heart of $HCN4^{R669Q/R669Q}$ embryos (left: PPc73K; middle: SHG-1E5; right: overlay; bar: 20 μm). (**B**) Western blot analysis of membrane proteins from Flp-In-293 cells, expressing HCN4 (left) or $HCN4^{R669Q}$ (right), labelled with the HCN4-β antibody. NT: non-transfected cells, +: treatment with PNGase F. (**C**) Left, upper panel: lysates from HEK293-mHCN1 cells. The following antibodies have been used to show the isoform specificity: 1, HCN4-β; 2, HCN4-specific PG2-7H9; 3, HCN1-specific RTQ-7C3. Middle, upper panel: lysates from HEK293-mHCN2 cells. Antibodies used: 4, HCN4-β; 5, HCN4-specific PG2-7H9; 6, HCN2-α. Right, upper panel: lysates from HEK293-mHCN4 cells. Antibodies used: 7, HCN4-β; 8, HCN4-specific PG2-7H9. All lower panels: loading control with anti-actin antibody. (**D**) Upper panel, lanes 1 and 2: membrane proteins from Flp-In-293 cells (1, non-transfected; 2, transfected with mHCN4) labelled with the HCN4-specific antibody PG2-7H9 (exposure time: 1 min). Lanes 3–5: total proteins from embryonic hearts (3, $HCN4^{+/+}$; 4, $HCN4^{+/R669Q}$; 5, $HCN4^{R669Q/R669Q}$; 10 hearts per genotype) labelled with PG2-7H9 (exposure time: 10 min). Lower panel: loading control with anti-actinin antibody. (**E**) Basal embryonic heart rate at E9.5, E10.5, and E11 ($HCN4^{+/+}$, red; $HCN4^{+/R669Q}$, green; $HCN4^{R669Q/R669Q}$, blue). The number of embryos analysed is indicated. Student's *t*-test: $^{*}P<0.05$ compared to $HCN4^{+/+}$ at the same developmental stage; $^{\Phi}P<0.05$ compared to the same genotype at E9.5. (**F**) Effect of isoproterenol (2 μM) on the embryonic heart rate ($HCN4^{+/+}$, red; $HCN4^{+/R669Q}$, green; $HCN4^{R669Q/R669Q}$, blue). Data have been normalized to the rates during superfusion with BM. (**G**) Increase in heart rate (at 9 min) during perfusion with isoproterenol. Data have been normalized to the corresponding heart rate during superfusion with BM (grey, basal heart rate; yellow, heart rate at 9 min). Statistical analysis: student's *t*-test; $^{*}P<0.05$ compared to basal heart rate; $^{\Phi}P<0.05$ compared to heart rate of the other genotypes at 9 min. (**H**) See F for NKH477 (100 μM). (**I**) See G for NKH477. Data represent mean±s.e.m.

The I_f of HCN4$^{R669Q/R669Q}$ cardiomyocytes activates slower and deactivates faster

To characterize genotypic differences of cardiomyocytes, we recorded I_f currents and action potentials from cultured cells of HCN4$^{+/+}$, HCN4$^{+/R669Q}$, and HCN4$^{R669Q/R669Q}$ embryonic hearts. Isolated beating cells were studied with the patch-clamp technique in the *whole-cell* configuration. The I_f current was activated by hyperpolarizing voltage steps from a holding voltage of −55 mV to test voltages up to −135 mV. Subsequently, a voltage step to −95 mV was ap-

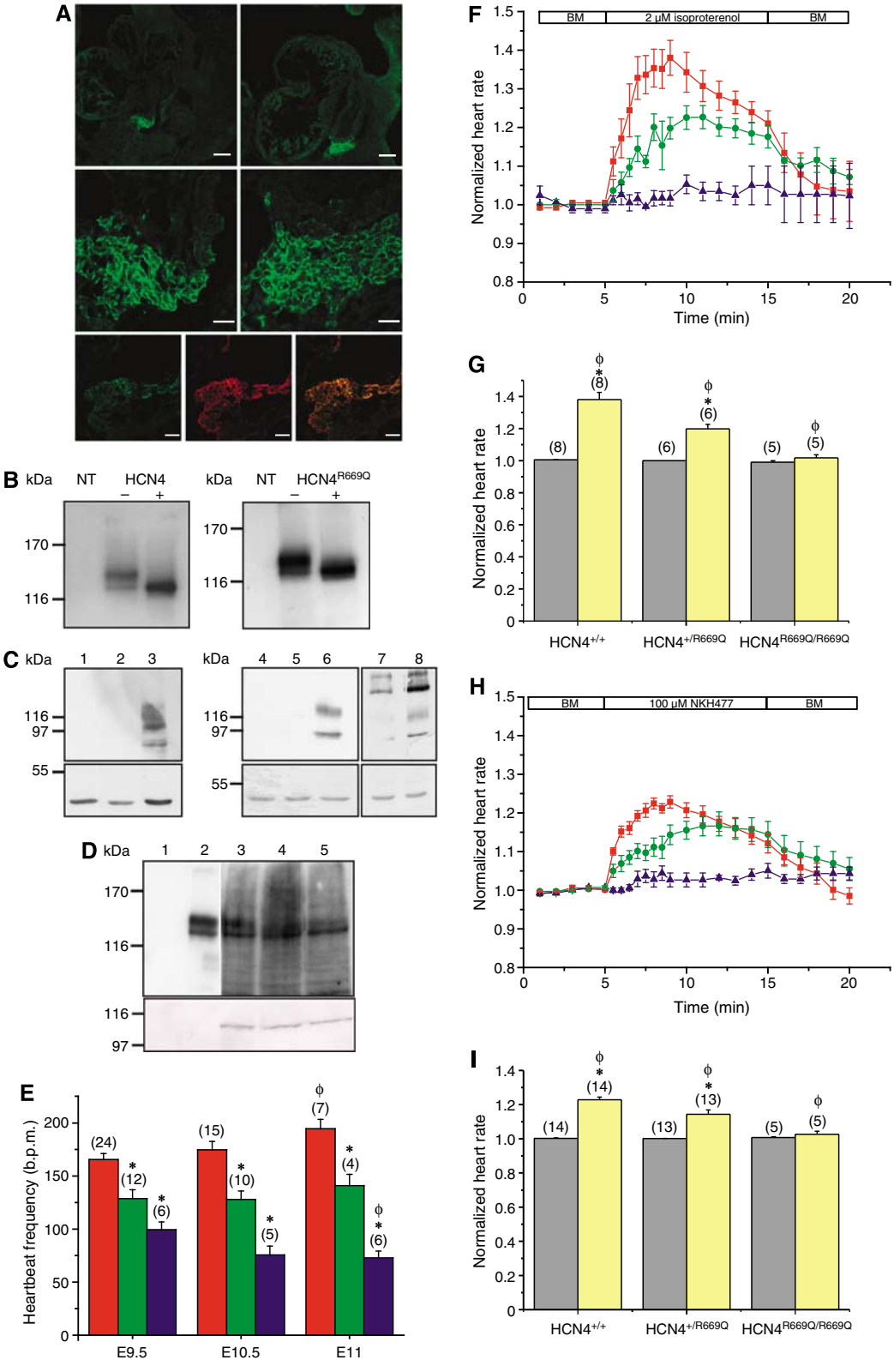

Table I Basal embryonic heart rate

	Basal heart beat (b.p.m.)		
	E9.5	E10.5	E.11
$HCN4^{+/+}$	164.5±5.9	174.6±7.8	194.5±8.7
$HCN4^{+/R669Q}$	129.7±9.0	127.9±7.9	141±10.5
$HCN4^{R669Q/R669Q}$	99.3±7.3	75.6±8.2	72.2±6.5

plied to probe the activation state of HCN channels. We observed robust I_f currents in all three genotypes. Figure 3A and B shows currents from cardiomyocytes of wild-type and homozygous embryos, respectively. The I_f current of wild-type cardiomyocytes activated faster and more completely than that of $HCN4^{R669Q/R669Q}$ cells (Figure 3A and B). Therefore, we analysed the kinetics of I_f current activation and deactivation in more detail. Figure 3C shows current responses of wild-type and homozygous cells to steps from the holding voltage (−55 mV) to the test voltage (−95 mV) and back to the holding voltage. We fitted simple exponential models to the respective current traces ignoring the initial delay at the onset of activation (see Figure 3C). While for the homozygous genotype a single exponential with a time constant of 1757±132 ms ($n=16$) was sufficient to describe activation, two time constants of 264±35 ms (relative amplitude 0.35) and 1771±474 ms (relative amplitude 0.65) ($n=11$) were necessary to describe wild-type currents. Similarly, deactivation of homozygous currents was well described by a single time constant of 172±23 ms ($n=9$), while for wild-type currents two time constants of 200±38 and 1690±314 ms ($n=8$) were necessary for a satisfactory fit. The additional time constant for wild-type currents was fast in the case of activation and slow in the case of deactivation, demonstrating that in wild type, currents activated faster and deactivated slower compared to currents of homozygous cells. Table II summarizes the results of the kinetic analysis. We have included in Table II also the kinetic analysis of the activation of heterologously expressed HCN4 and $HCN4^{R669Q}$ channels. The activation properties of wild-type cardiomyocytes are strikingly similar to those of heterologously expressed HCN4 currents in the presence of cAMP (see Table II).

The voltage-dependent activation of I_f in cardiomyocytes differs among genotypes

Next, we analysed tail currents as in Figure 3A and B to determine the voltage dependence of activation of I_f for the different genotypes. The voltage of half-maximal activation ($V_{1/2}$) in the three genotypes differed significantly: $V_{1/2}$ was −82.5±3.2 mV ($n=12$) for wild-type, −89.3±6.6 mV ($n=12$) for heterozygous, and −95.7±4.5 mV ($n=9$) for homozygous cardiomyocytes (Figure 3D). This result is reminiscent of the differences observed with heterologously expressed HCN4 and $HCN4^{R669Q}$ channels in the presence of cAMP (compare Figure 2A). However, for the experiments presented here, no exogenous cAMP was added. We interpret this result to indicate that even in the unstimulated state, the I_f in wild-type and heterozygous cardiomyocytes is significantly upregulated by cAMP.

Isolated $HCN4^{R669Q/R669Q}$ cardiomyocytes beat with lower frequencies

We recorded action potentials from isolated cells of wild-type and homozygous hearts to investigate whether the differences in I_f are reflected in the spontaneous rates of cardiomyocytes. Action potentials were highly variable from cell to cell, indicating that cardiomyocytes at this developmental stage have already undergone substantial differentiation. Spontaneous rates of $HCN4^{+/+}$ cells ranged from 60 to 337 b.p.m. (Figure 3E, upper panel), the action potential duration (APD) varied from 30 to 360 ms, and the MDP varied from −62 to −87 mV. Rates from $HCN4^{R669Q/R669Q}$ cells varied from 15 to 225 b.p.m. (Figure 3E, lower panel), ADPs from 5 to 800 ms, and MDPs from −61.5 to −87 mV. On average, rates were significantly lower in $HCN4^{R669Q/R669Q}$ cells (99±11 b.p.m. ($n=32$)) than in $HCN4^{+/+}$ cells (156±11 b.p.m. ($n=37$), $P<0.05$). We reasoned that cells with the highest spontaneous rates eventually pace the embryonic heart. In wild-type embryos, we identified pacemaker-like cardiomyocytes (9 of 32 cells) with particularly high average rates of 211±20 b.p.m. ($n=9$), MDPs of −75.7±0.7 mV, APDs < 100 ms, and robust I_f currents when voltage clamped. In the presence of cAMP (100 μM in the pipette solution), this cell population displayed beat frequencies of 338±41 b.p.m., indicating a pronounced stimulatory effect of cAMP. Action potentials of a typical wild-type cell from this population are shown in Figure 3F (upper panel). The cell is spontaneously active at about 240 b.p.m.

We then searched for $HCN4^{R669Q/R669Q}$ cells that produced the same action potential shape (APD < 100 ms) characteristic of this particular class of cells. In total, 8 of 32 cells were found with action potential shapes similar to the ones we were looking for. These cells were characterized by a relatively slow rate of 92±9 b.p.m. ($n=8$) and MDPs of −82.6±0.7 mV. Figure 3F (middle panel) shows a typical example. The cell was active with 75 b.p.m. and had an MDP of −83 mV. When we injected a depolarizing current of 20 pA into this cell (Figure 3F, lower panel) to compensate for the poor activation of the $HCN4^{R669Q/R669Q}$ channel, action potential rates increased drastically to values otherwise not observed in $HCN4^{R669Q/R669Q}$ cells. Under these conditions, rate, action potential shape, and MDP were very similar to the wild-type pacemaker cell types at this developmental stage.

The I_f of $HCN4^{R669Q/R669Q}$ cardiomyocytes is unresponsive to changes in cAMP

We next studied I_f currents in the presence of exogenous cAMP (500 μM). Under this condition, the $V_{1/2}$ value of I_f currents from wild-type cardiomyocytes was further shifted by 6 to −76.2±2.9 mV ($n=6$), while that from homozygous cardiomyocytes was largely unchanged ($V_{1/2}=92.3\pm4.9$ mV, $n=6$) (Figure 3G). The small shift of $V_{1/2}$ by 6 mV in wild-type cells compared to a shift by 24 mV for heterologously expressed HCN4 channels supports the notion that the level of cAMP in cardiomyocytes is unusually high in the resting state. Therefore, the dynamic range of changes in cAMP is restrained and the extent of regulation of I_f is accordingly smaller.

We reasoned that inhibition of basal adenylyl cyclase activity should abolish the genotypic differences in $V_{1/2}$. Muscarinic modulation is known to inhibit adenylyl cyclase. We stimulated cells with carbachol (10 μM in the bath solution) and studied the effect on I_f currents in wild-type

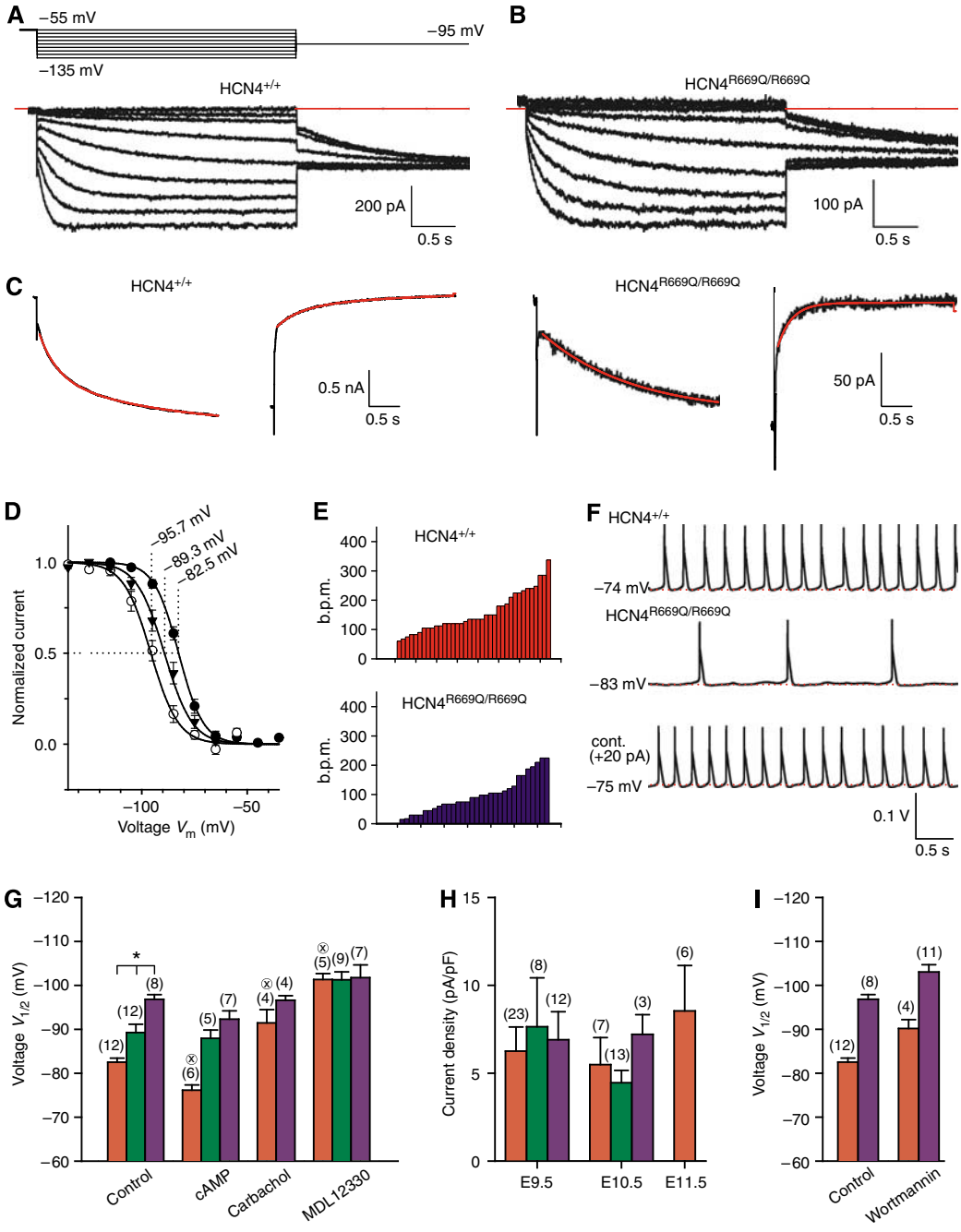

Figure 3 I_f currents and action potentials recorded from isolated embryonic cardiomyocytes. (**A**) Upper panel: voltage protocol for the recording of I_f. Lower panel: I_f current in an HCN4$^{+/+}$ cell. Tail currents at −95 mV were used to analyse the voltage dependence of activation. The red line in the current progression indicates the zero current level. (**B**) I_f current in an HCN4$^{R669Q/R669Q}$ cell. The red line in the current progression indicates the zero current level. (**C**) Left part: activation and deactivation of HCN4$^{+/+}$ channels. Right part: activation and deactivation of HCN4$^{R669Q/R669Q}$ channels. The time course of activation and deactivation of I_f was fitted with two (HCN4$^{+/+}$) or a single (HCN4$^{R669Q/R669Q}$) exponential term (red traces). (**D**) Voltage-dependent activation of I_f from HCN4$^{+/+}$ (filled circles), HCN4$^{+/R669Q}$ (filled triangles), and HCN4$^{R669Q/R669Q}$ (open circles) cells. The solid line was calculated with the Boltzmann equation with the following parameters (mean ± s.d.): HCN4$^{+/+}$, $V_{1/2} = -82.5 \pm 3.2$ mV and $s = 5.8 \pm 2.4$ mV ($n = 12$); HCN4$^{+/R669Q}$, $V_{1/2} = -89.3 \pm 6.6$ mV and $s = 6.6 \pm 1.1$ mV ($n = 12$); HCN4$^{R669Q/R669Q}$, $V_{1/2} = -95.7 \pm 4.5$ mV and $s = 6.5 \pm 2.6$ mV ($n = 9$). (**E**) Summary of beat frequencies (in b.p.m.) of isolated cells recorded in current-clamp mode. Upper panel: frequencies recorded from HCN4$^{+/+}$ cells. Lower panel: frequencies recorded from HCN4$^{R669Q/R669Q}$ cells. (**F**) Action potentials of an HCN4$^{+/+}$ (upper panel) or an HCN4$^{R669Q/R669Q}$ (middle and lower panels) cell. In the experiment shown in the lower panel, a depolarizing current of 20 pA was injected. (**G**) Voltages $V_{1/2}$ of half-maximal activation of HCN4$^{+/+}$ (red), HCN4$^{+/R669Q}$ (green), and HCN4$^{R669Q/R669Q}$ (blue) under control conditions, with 500 μM cAMP (HCN4$^{+/+}$ and HCN4$^{R669Q/R669Q}$) or 100 μM cAMP (HCN4$^{+/R669Q}$) in the pipette solution, or with 10 μM carbachol in the bath, or with 10 μM MDL12330 in the pipette solution. (**H**) Current densities at −135 mV (determined as I_f, −135 mV per cell capacitance) of cells from HCN4$^{+/+}$ (red), HCN4$^{+/R669Q}$ (green), and HCN4$^{R669Q/R669Q}$ (blue) embryonic hearts at defined developmental stages. Recordings were made between 24 and 36 h after preparation. (**I**) Voltages $V_{1/2}$ of half-maximal activation of I_f from HCN4$^{+/+}$ (red) and HCN4$^{R669Q/R669Q}$ (blue) cells under control conditions (data from G) and from cells pre-incubated with wortmannin (10 μM) for at least 30 min. Data represent mean ± s.e.m. except when explicitly stated; $^*P < 0.05$ as indicated; $^{\otimes}P < 0.05$ compared to the same genotype under control conditions.

Table II Kinetics of I_f activation and deactivation

	τ_{fast} (ms)	Relative amplitude $A_1/(A_1+A_2)$	τ_{slow} (ms)	Relative amplitude $A_2/(A_1+A_2)$	*n*
Activation					
HCN4[a]	—	—	1873±132	1.0	19
HCN4 (100 μM cAMP)[a]	290±32	0.55±0.09	1522±426	0.45±0.09	7
$HCN4^{R669Q}$ [a]	—	—	1749±185	1.0	9
$HCN4^{+/+}$ [b]	264±35	0.35±0.03	1771±474	0.65±0.03	11
$HCN^{R669Q/R669Q}$ [b]	—	—	1757±132	1.0	16
Deactivation[b]					
$HCN4^{+/+}$	200±38	0.43±0.04	1690±314	0.57±0.04	8
$HCN^{R669Q/R669Q}$ [b]	172±23	1.0	—	—	9

[a]Recorded in HEK293 cells.
[b]Genotype of embryonic cardiomyocytes.
The equation $I(t) = A_0 + A_1\exp(-t/\tau_{fast}) + A_2\exp(-t/\tau_{slow})$ was used to describe the activation and deactivation of hyperpolarization activated currents (A_1 and A_2, amplitudes of the fast and slow components, respectively; τ_{fast} and τ_{slow}, fast and slow time constants, respectively).

and homozygous cardiomyocytes. While I_f of homozygous cardiomyocytes was unaffected by carbachol, some wild-type cells displayed I_f with a more negative activation curve. However, the action of carbachol was variable (range of $V_{1/2}$ of wild-type I_f from −84 to −98 mV), indicating that the muscarinic system may not be homogeneously expressed in all cardiomyocytes. Consequently, we used the adenylyl cyclase inhibitor MDL12330 (10 μM in the pipette solution) to directly inhibit cAMP synthesis in cardiomyocytes. In the presence of MDL12330, all genotypes displayed the same $V_{1/2}$ of −101 mV (Figure 3G). This result strongly supports the notion that a high resting cAMP level is responsible for the differences in I_f and, accordingly, for the differences in heart rate between the three genotypes.

I_f current densities do not differ among genotypes

Some mutations in the CNBD of HERG channels have been proposed to induce trafficking defects, that is, fewer channels are incorporated into the plasma membrane (for review, see Thomas *et al*, 2003). To investigate whether Arg669 is also important for trafficking, we determined I_f current densities of embryonic cardiomyocytes at different developmental stages. We used the time-resolved component of I_f at −135 mV (full activation) for this analysis. Figure 3H summarizes the results. We observed no significant genotypic differences of I_f current density at days E9.5 or E10.5. Furthermore, no significant increase of I_f current density was observed in wild-type cells from E9.5 to E11.5, indicating that the increase of heart rate observed during this developmental window is probably not caused by an enhanced expression of I_f currents. HCN currents have been shown to exhibit an instantaneous current component (Gauss *et al*, 1998; Macri and Accili, 2004; Mistrik *et al*, 2006; Proenza and Yellen, 2006; Lin *et al*, 2007). We determined the current density of the instantaneous current (including leak) at −95 mV for the three genotypes. We observed no genotypic differences (mean (median) ± s.d. (number of experiments); wild-type, 2.5 (1.8) ± 2.5 pA/pF ($n = 38$); $HCN4^{+/R669Q}$, 1.8 (1.6) ± 1.3 pA/pF ($n = 24$); $HCN4^{R669Q/R669Q}$, 2.0 (2.0) ± 1.3 pA/pF ($n = 15$)).

PI_3 kinase is not responsible for the genotypic differences of I_f

Finally, we studied whether I_f currents of wild-type and homozygous cardiomyocytes are differently regulated by phosphoinositide 3 (PI_3) kinase. Recently, it has been shown that PIP_2 can act as a ligand that allosterically opens HCN channels by shifting the activation curve to more positive potentials (Pian *et al*, 2006; Zolles *et al*, 2006). We studied the activation of I_f after incubation of cardiomyocytes with wortmannin (10 μM in the bath solution) for at least 30 min. While the $V_{1/2}$ values of both, wild type and $HCN4^{R669Q/R669Q}$, were shifted to more negative values by wortmannin treatment (7.7 and 6.2 mV, respectively), the difference of $V_{1/2}$ among genotypes was unchanged (Figure 3I). We conclude that there is no differential regulation of wild type and mutant I_f by PI_3 kinase. Taken together, our results indicate that wild-type I_f is enhanced by cAMP at rest and that this acceleration is indispensable for pacemaker activity of I_f.

Heart rates in adult mice do not differ between genotypes

The differences in basal heart rate and in the activation of I_f between wild-type and heterozygous embryos prompted us to study the heart rate in freely moving adult $HCN4^{+/+}$ and $HCN4^{+/R669Q}$ mice by telemetric recording of electrocardiogram (ECG). Neither the heart rate at rest nor during exercise or mental stress was different between genotypes (Figure 4A and C). The heart rate of sedated animals and the intrinsic rate of the isolated heart were also not different between genotypes (Figure 4B and C), nor was the electrophysiology of the AV node and the ventricle (Figure 4C). After exercise, $HCN4^{+/R669Q}$ mice developed pauses and sino-atrial block more often than their wild-type littermates ($HCN4^{+/R669Q}$: 9±7 pauses/55 min, median 6.5, range 2–25; $HCN4^{+/+}$: 6.5±5 pauses/55 min, median 1, range 0–14, $P<0.05$). Sino-atrial block and sinus pauses were also found in spontaneously beating, Langendorff-perfused hearts, mostly during washout of the β-adrenoceptor agonist orciprenaline (baseline: pauses in 4/10 $HCN4^{+/R669Q}$ hearts versus 1/9 $HCN4^{+/+}$ hearts; during orciprenaline infusion: pauses in 5/10 $HCN4^{+/R669Q}$ versus 1/9 $HCN4^{+/+}$ hearts; during washout of orciprenaline: pauses in 8/10 $HCN4^{+/R669Q}$ versus 0/9 $HCN4^{+/+}$ hearts, $P<0.05$ for $HCN4^{+/R669Q}$ versus $HCN4^{+/+}$).

Discussion

The role of I_f in embryonic and adult cardiomyocytes is a matter of a long-lasting debate (Kodama *et al*, 2002; Lipsius and Bers, 2003). While some groups favour I_f as the principle

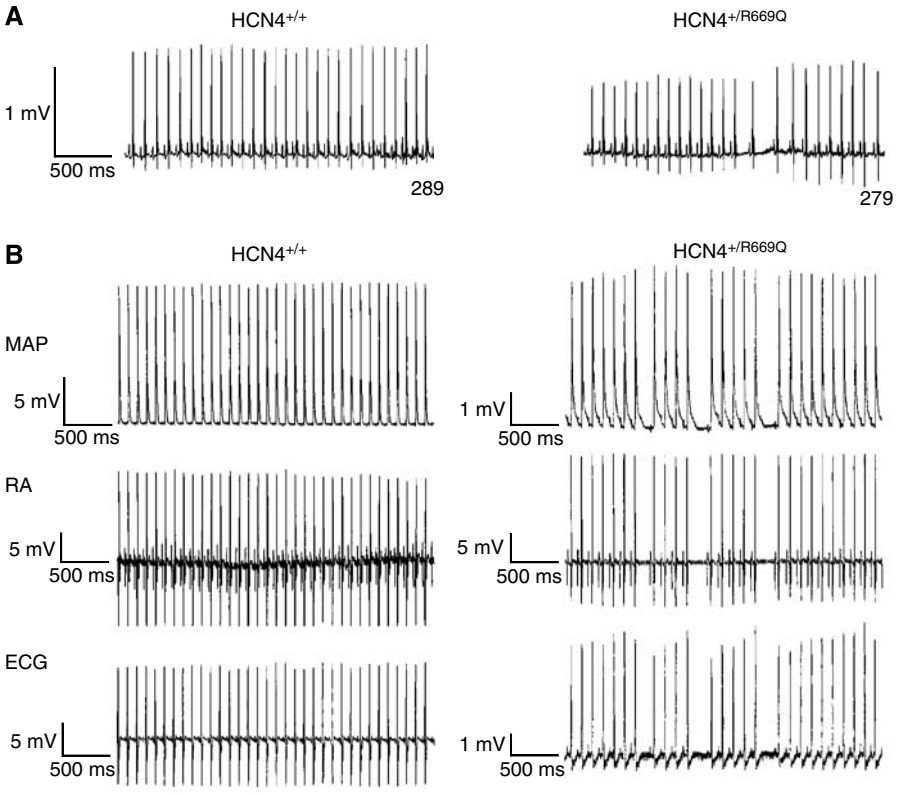

C

	HCN4$^{+/+}$	HCN4$^{+/R669Q}$	HCN4$^{+/+}$	HCN4$^{+/R669Q}$
ECG in sedated animals	*n*=8	*n*=8		
Heart rate	446±85	416±50		
PQ interval (ms)	39±2	39±4		
QT interval (ms)	61±14	59±3		
QTc (m/s$^{1/2}$)	51±7	49±2		
	Normal activity		**Swimming**	
ECG in freely moving animals	*n*=5	*n*=6	*n*=5	*n*=6
Heart rate (b.p.m.)	542±96	418±45	712±25	710±20
Maximal heart rate (b.p.m.)	869±80	787±247	919±43	934±31
Minimal heart rate (b.p.m.)	297±45	265±42	423±54	416±30
PQ interval (ms)	37±2	39±2	ND	ND
	Baseline		**Orciprenaline (1.7 μM)**	
Electrophysiology in the isolated heart	*n*=9	*n*=10	*n*=9	*n*=10
Intrinsic heart rate (b.p.m.)	405±44	412±38	620±26	531±46
Wenckebach point (ms)	83±2	85±5	70±4	67±3
Ventricular APD at 70% repolarization (ms)	20±9	17±5	15±5	9±4

Figure 4 HCN$^{+/R669Q}$ mice display a sino-atrial block. (**A**) Representative examples of telemetric ECG recordings in freely moving mice carrying an implanted ECG transmitter. All recordings were obtained during the 55-min recovery period after stress tests (air jets or swimming). Animal numbers are indicated. (**B**) Representative recording of spontaneous rhythm in isolated, Langendorff-perfused hearts. Ventricular monophasic action potential (MAP), right atrial electrogram (RA), and lead II of the tissue bath ECG (ECG) are shown. The WT heart shows a constant sinus rhythm, the HCN4$^{+/R669Q}$ heart shows three pauses with doubling of cycle length, consistent with sino-atrial block. (**C**) Electrophysiological measurements in sedated animals, freely moving animals and in the isolated, beating heart. All values are given as mean±s.e.m. There were no significant differences among groups. Rates in the isolated hearts include hearts with sino-atrial block. This explains the relatively large s.d. in this group during orciprenaline treatment.

pacemaker current of SAN cells, others attribute only a minor modulatory function to this current. We studied here knock-in mice that carry a single amino-acid exchange in the CNBD of the HCN4 channel, which represents the major component of the I_f current in SAN cells (Stieber *et al*, 2003). Our results provide the following insights.

First, hearts from HCN4$^{R669Q/R669Q}$ embryos show virtually no response to catecholaminergic stimulation, indicating that the HCN4 channel is the major if not only target for cAMP-mediated acceleration of the heart rate by catecholamines. Furthermore, this result shows that protein phosphorylation by another important target of cAMP signalling, cAMP-dependent protein kinase, is not involved in cardiac pacemaking at this developmental stage. The β-adrenergic acceleration of the heart rate is crucial for survival of the embryo (Portbury *et al*, 2003; Chandra *et al*, 2006). Adrenergic stimulation maintains the embryonic heart rate during transient hypoxia that occurs during gestation. Hypoxia induces a life-threatening bradycardia unless catecholamine release compensatorily accelerates the heart rate (Portbury *et al*, 2003).

The fatal outcome of the HCN4$^{R669Q/R669Q}$ knock-in model demonstrates the outstanding role of HCN4 as the key transducer of catecholaminergic signalling in the embryonic heart ensuring survival of the embryo.

Another key observation of our study is that even in the absence of adrenergic stimulation, the rates of heterozygous

and homozygous hearts were significantly slower than those of wild-type hearts. This genotypic difference persisted in isolated cells where the I_f current displayed different activation properties: the activation curve of wild-type I_f was significantly shifted towards more positive voltages compared to that of homozygous cells. In heterozygous cells, this shift was smaller. The shift can be accounted for by high basal adenylyl cyclase activity resulting in high cAMP levels. Indeed, blocking adenylyl cyclase activity with MDL12330 completely eliminates differences in the activation curves of I_f. Moreover, Vinogradova *et al* (2006) have recently shown that the basal cAMP level in rabbit SAN cells is markedly higher than in other cardiac cell types. Finally, even in non-cardiac cells, namely GH(3) immortalized pituitary cells, basal cAMP levels significantly contribute to HCN channel activity (Kretschmannova *et al*, 2006).

One of the most striking observations was that the resting beat frequency of embryonic $HCN4^{R669Q}$ and $HCN4^{-/-}$ (Stieber *et al*, 2003) hearts did not differ. The $HCN4^{R669Q}$ channel, while present at similar density as the HCN4 channel in wild-type cardiomyocytes and proven functional, seems not to contribute to the pacing of the embryonic heart. Obviously, additional pacemaker mechanisms besides I_f must exist in the embryonic heart that are responsible for the residual heart rate found in homozygous embryos. We investigated the beating properties of wild-type and homozygous cells in detail. In $HCN4^{+/+}$ cells, we identified a cell type with especially high beating rates that we consider the pacemaker cells of the embryonic heart. A cell population with very similar action potentials was also found in the $HCN4^{R669Q/R669Q}$ preparation. In this respect, our knock-in mouse model differs from the HCN4 knockout model, in which no 'mature' pacemaker cells were found (Stieber *et al*, 2003). The rates of these 'pacemaker-like' $HCN4^{R669Q/R669Q}$ cells were much lower than those in wild-type cells. Indeed, other cell types of the $HCN4^{R669Q/R669Q}$ heart exhibited higher rates than this particular cell population. Most of these other cells displayed I_f currents, however, some were devoid of I_f. We speculate that in the $HCN4^{R669Q/R669Q}$ heart probably these other cell populations take over to pace the heart, albeit with reduced rates.

If we assume that cells with I_f are involved in pacemaking, why are the rates of $HCN4^{R669Q/R669Q}$ and $HCN4^{-/-}$ identical? First, the MDP of most of the cells recorded here adopts values of about −75 mV. At this voltage the open probability of the $HCN4^{R669Q}$ channel is only ∼4%, as determined from the voltage dependence of activation. Most likely, the depolarizing action of the $HCN4^{R669Q/R669Q}$ channel is too small to be of any significance. The channel, in the absence of cAMP, becomes physiologically silent. Second, in $HCN4^{-/-}$ as well as $HCN4^{R669Q/R669Q}$ embryos other mechanisms may compensate the effect of the deletion or mutation of the HCN4 channel. This is expected to result in the same heart rate in both mouse lines. However, other HCN channel isoforms are not upregulated in HCN4 knockout mice (Stieber *et al*, 2003; Herrmann *et al*, 2007) and other potential mechanisms have not been studied so far.

In light of these findings and models of heart-rate regulation in the SAN (Robinson *et al*, 2006), the normal heart rate of adult heterozygous $HCN4^{R669Q}$ mice at rest and during exercise is unexpected. While hearts of heterozygous embryos display significantly reduced rates and attenuated responses to catecholamines, no such genotypic differences exist in adult hearts. Different scenarios can be envisioned to interpret this result. First, during development, other pacemakers may compensate the bradycardic effect of the channel mutation. In humans, the situation might be different. Mutations in or near the CNBD of HCN4 have been found to lead to a profound bradycardic phenotype in humans (Schulze-Bahr *et al*, 2003; Milanesi *et al*, 2006). The molecular phenotype of one of these mutations was somewhat milder than the one investigated here. The mutated channels in this study are activated at more negative voltages than wild-type channels (Milanesi *et al*, 2006). Interestingly, the negative shift of $V_{1/2}$ was only 8.4 mV, less than the shift we observed for the I_f in homozygous cardiomyocytes (13 mV). Thus, a putative compensatory mechanism is lacking in humans. While a compensatory mechanism cannot be discarded, we favour a different interpretation of the identical heart rates in wild-type and heterozygous mice. During embryonic development of the mouse, the role of I_f may switch from that of a major pacemaker to one that backs up other pacing elements in the adult. In fact, while this manuscript was in preparation, Herrmann *et al* (2007) published their work on a mouse model in which the HCN4 channel has been deleted cardiac specifically in adult mice. Mutant mice showed no defect in heart-rate regulation during sympathetic stimulation, but exhibit cardiac arrhythmia characterized by sinus pauses. The phenotype is similar to that of adult heterozygous $HCN4^{+/R669Q}$ mice. It will be interesting to investigate the cardiac phenotype of adult homozygous $HCN4^{R669Q/R669Q}$ mice to study whether these animals display the phenotype observed in knockout mice. This experiment would test the idea whether cAMP binding is indispensable for the physiological function of HCN4 channels rather than only modulatory. From our results and the similar observation of Herrmann *et al* (2007), we conclude that in adult mice, HCN4 channels serve a back-up mechanism that maintains a stable heart beat in situations during and after stress. HCN4 channels are probably no longer involved in sympathetic stimulation of the heart rate.

In humans, the role of HCN4 obviously is different. How can we explain these species-dependent differences? The most obvious difference in cardiac function between mice and humans is the frequency of the beating heart (60–200 b.p.m. in humans versus 500–1000 b.p.m. in mice). The beating frequency in humans is similar to the one in embryonic mice, where we have shown that HCN4 is a true pacemaker. We suggest that HCN4 can only serve as pacemaker at low beating frequencies; at higher frequencies, its slow activation characteristics are not suitable to support higher heart rates.

Materials and methods

Cloning of the targeting vector for the generation of HCN4 knock-in mice

A genomic clone containing exons IV–VIII of the HCN4 gene was isolated from a mouse genomic 129/SvJ library (Stratagene, Amsterdam, The Netherlands). The library was probed with a cDNA fragment encoding the S5 to S6 region of mHCN4. A clone of roughly 11.7 kb was subcloned into pBluescript SK(−) (Stratagene), sequenced, and used for the construction of the targeting vector. The vector was constructed in neo-flox-8 by using a 1.8-kb genomic fragment as short arm of homology and a 4.4-kb genomic fragment as long arm of homology. The short arm was generated by ligating

an *Aat*II/*Hin*dIII fragment of the genomic clone together with a *Hin*dIII/*Xba*I-digested PCR product (forward: 5′-TCAGAAGCTTG GAGGGACCC-3′; reverse: 5′-CCACTtctAGAACCCTCAATGGAA-3′) into the *Aat*II/*Xba*I-digested neo-flox-8. The long arm was generated by ligating an *Sph*I/*Nsi*I fragment of the genomic clone with a *Not*I/*Asp*718-digested PCR product (forward: 5′-TCTCA GATGGCgGccgcAGCACTTGTGTT-3′; reverse: 5′-ACTGGGTACCA GCAGCACCC3′) as well as an *Asp*718/*Sph*I-digested PCR product that carries the mutation CG to AG in exon VII into the *Not*I/*Nsi*I-digested neo-flox-8 containing the short arm. The mutated PCR fragment was generated by subcloning an *Asp*718/*Nar*I fragment into pBluescript SK(−) and using this subclone as a template for a recombinant PCR performed with the 'QuikChange site-directed mutagenesis kit' (Stratagene) (forward: 5′-GACCCGGGGTCGGCa gACAGCCAGCGTCAG-3′; reverse: 5′-CTGACGCTGGCTGTctGCC-GACCCCGGGTC-3′). For negative selection, a diphtheria toxin A (DTA) cassette was inserted at the 5′ end of the short arm. The DTA cassette has been amplified on pGEMTeasyDTA2 (forward: 5′-AATGACGTCCGGTACCTCGACG-3′; reverse: 5′-ACTGACGTCCG GTACCTTAATTAA-3′) and subcloned into pBluescript. An *Aat*II fragment was excised and cloned into the *Aat*II site of the targeting vector.

Generation of HCN4 knock-in mice

The vector was linearized with *Nsi*I and electroporated into V6.5 embryonic stem cells (Rideout *et al*, 2000). Positive clones were identified by Southern blot analysis with 5′ and 3′ probes. Blastocyst injection was performed for three independent clones. Male chimeras were crossed with C57BL/6J females (Jackson Laboratories, Bar Harbor, ME, USA). The neomycin resistance gene was removed by crossing heterozygous mice with deleter-cre mice (Schwenk *et al*, 1995). Heterozygous mice were backcrossed for 10 generations to a C57BL/6J background.

Embryos were genotyped by PCR of yolk-sac DNA, and mice by PCR of tail DNA using the following primer set: primer no. 1: 5′-CTTAGTGGTAGACTGTTGTGGTT-3′ and primer no. 2: 5′-GCTGG CTGTGCGCCGACCC-3′ amplifying a 586-bp wild-type fragment, primer no. 3: 5′-TCTGACGCTGGCTGTCTG-3′ and primer no. 4: 5′-CCATTGAGGGTTCTAGACTC-3′ amplifying a 1804-bp fragment in $HCN4^{+/neoR669Q}$ mice and a 610-bp fragment after excision of the neomycin resistance gene.

Isolation and culture of embryonic hearts and cardiomyocytes

Embryos from timed matings were removed from pregnant females and transferred to pre-warmed PBS (in mM): NaCl 137; KCl 2.7; Na_2HPO_4 10; and KH_2PO_4 1.8. For analysis of the beat frequency, hearts were dissected, placed into DMEM (Gibco, Karlsruhe, Germany) containing 10% FBS (Gibco), and cultured over night at 37°C, 10% CO_2. During measurements, hearts were superfused with DMEM containing 10 mM HEPES/NaOH pH 7.4 (basal medium, BM). Drugs were added to BM (isoproterenol: 2 μM; NKH477: 100 μM). For isolation of cardiomyocytes, hearts were dissected and placed in a solution containing (in mM): NaCl 120, KCl 5.4, $MgSO_4$ 5, sodium pyruvate 5, taurine 20, HEPES 10, glucose 20, $CaCl_2$ 0.03, and 1 mg/ml collagenase B (Roche Diagnostics, Mannheim, Germany). The incubation was stopped with DMEM containing 20% FBS, 1% non-essential amino acids (Gibco), 1% penicillin/streptomycin (Gibco), and 100 μM β-mercaptoethanol (Sigma, Seelze, Germany). Cardiomyocytes were placed in a shaker at 37°C for 30 min, plated onto 3 cm dishes, and incubated at 37°C, 5% CO_2 for 24–72 h.

Western blot analysis and immunohistochemistry

Ten embryonic hearts from each genotype were pooled and homogenized in lysis buffer (in mM): NaCl 10, EDTA 2, HEPES 25, DTT 3, supplemented with 0.5 mg/ml Pefabloc SC. HEK293 cells were lysed in lysis buffer (in mM): Tris–HCl (pH 7.6) 10, NaCl 140 and 1% Triton X-100, supplemented with 0.5 mg/ml Pefabloc SC. Membrane proteins from Flp-In-293mHCN4 and Flp-In-$293mHCN4^{R669Q}$ cells were isolated as described (Wachten *et al*, 2006). Proteins were separated on a 7.5% SDS–PAGE, blotted, and probed with one of the following antibodies: monoclonal HCN4-specific antibody (PG2–7H9, rat, 1:2) (Harzheim, 2006; Mataruga, 2006), polyclonal, affinity-purified HCN4-specific antibody (HCN4-β, rabbit, 1:2000) (Mataruga, 2006), monoclonal HCN1-specific antibody (RTQ-7C3, rat, 1:100) (Scholten, 2001), polyclonal, affinity-purified HCN2-specific antibody (HCN2-α, rabbit, 1:1000) (Mataruga, 2006) by using a chemiluminescence detection system. For reprobing with either a monoclonal α-actinin antibody (sarcomeric, mouse; Sigma, 1:1000) or a polyclonal anti-actin antibody (rabbit; Sigma, 1:200) the membranes were incubated in stripping buffer (in mM): Tris–HCl (pH 6.7) 62.5, β-mercaptoethanol 100, and 2% SDS for 30 min at 65°C, washed with PBS and probed again. For immunohistochemical analysis, embryos were fixed in 5% paraformaldehyde, cryo-protected in 10 and 30% sucrose, and embedded in Tissue Tek (Sakura Finetek, Zoeterwoude, The Netherlands) at −20°C. Frozen sections (16 μm, sagittal) were pre-incubated in blocking buffer (PBS, 0.5% Triton X-100, 5% Chemiblocker). Sections were incubated with the HCN4-specific antibodies (SHG-1E5: monoclonal, rat, 1:5: PPc73K: polyclonal, rabbit, 1:400 (Scholten, 2001)) overnight and with the secondary antibodies (Alexa Fluor 488 goat anti-rat IgG; Molecular Probes, Karlsruhe, Germany; CY3 donkey anti-rabbit IgG, 1:500; Dianova, Hamburg, Germany) for 1 h in phosphate buffer containing 5% Chemiblocker. The labelled cryo-sections were analysed with a confocal laser-scanning microscope (Leica TCS, Solms, Germany).

Electrophysiological measurements

We recorded from cells with the patch-clamp technique in the whole-cell configuration. The pipette solution contained (in mM): K^+ aspartate 130, NaCl 10, $MgCl_2$ 2, EGTA 1, HEPES 10, pH 7.2 (KOH). cAMP or MDL12330 was added to the pipette solution as indicated. Cardiomyocytes were bathed in BM. Wortmannin or carbachol were added to BM as indicated. Flp-In-293 cells expressing HCN4 and $HCN4^{R669Q}$ channels were bathed in a solution containing (in mM): NaCl 140, KCl 5.4, $CaCl_2$ 1.8, $MgCl_2$ 1, HEPES 5, glucose 10, pH 7.4 (NaOH). All recordings were performed at 37°C. All voltages given were corrected for liquid junction potentials.

ECG and telemetry

Six-lead surface ECGs were recorded in littermate pairs of mice (12 weeks old) during isoflurane inhalation (1–1.5%). Recordings of 10 s were used for signal averaging. To record an ECG in freely roaming animals, a telemetric ECG transmitter (DSI, St Paul, MN, USA) was implanted. The telemetric ECG was analysed during normal activity and periods of stress, that is, swimming and warm air jets, according to published protocols (Kirchhof *et al*, 2003, 2006; Knollmann *et al*, 2003; Fabritz *et al*, 2004). All recordings were digitized (EMKA, Falls Church, VA, USA) at 2 kHz and analysed off-line.

Electrophysiological study of the isolated heart

To assess intrinsic heart rate and AV nodal conduction, the heart was rapidly excised and retrogradely perfused in a Langendorff apparatus. Ventricular monophasic action potentials, atrial and ventricular electrograms, and tissue bath ECGs were simultaneously recorded during spontaneous rhythm and during programmed atrial stimulation (incremental atrial pacing, constant pacing at 100 and 140 ms cycle length) at baseline and during perfusion with orciprenaline (1.7 μM) following published techniques (Kirchhof *et al*, 2003, 2006; Kuhlmann *et al*, 2006).

All original recordings were scrutinized for arrhythmias. We analysed heart rate, AV nodal conduction, APD, and QT interval semi-automatically using custom-designed software (LabVIEW and EMKA). Sino-atrial block (2:1) was defined following accepted prespecified clinical criteria, that is, a sudden two-fold increase of PP interval. All analyses were blinded to genotype.

Statistical analysis

Data are expressed as mean ± s.d. or mean ± s.e.m. Statistical comparisons were carried out with Student's *t*-test.

Acknowledgements

We thank J Deussing for providing the neo-flox-8 vector, A Mataruga and A Scholten for the generation and characterization of the HCN4-specific antibodies, and C Aretzweiler for superb technical assistance and help with the animals. DH was a fellow of the Boehringer Ingelheim Fonds, TB was supported by the Land Nordrhein-Westfalen, and PK is supported by the IZKF Münster.

References

Barbuti A, Baruscotti M, DiFrancesco D (2007) The pacemaker current: from basics to the clinics. *J Cardiovasc Electrophysiol* **18:** 342–347

Biel M, Schneider A, Wahl C (2002) Cardiac HCN channels: structure, function, and modulation. *Trends Cardiovasc Med* **12:** 206–212

Bogdanov KY, Vinogradova TM, Lakatta EG (2001) Sinoatrial nodal cell ryanodine receptor and Na^+–Ca^{2+} exchanger: molecular partners in pacemaker regulation. *Circ Res* **88:** 1254–1258

Bubis J, Neitzel JJ, Saraswat LD, Taylor SS (1988) A point mutation abolishes binding of cAMP to site A in the regulatory subunit of cAMP-dependent protein kinase. *J Biol Chem* **263:** 9668–9673

Bucchi A, Baruscotti M, Robinson RB, DiFrancesco D (2003) I_f-dependent modulation of pacemaker rate mediated by cAMP in the presence of ryanodine in rabbit sino-atrial node cells. *J Mol Cell Cardiol* **35:** 905–913

Chandra R, Portbury AL, Ray A, Ream M, Groelle M, Chikaraishi DM (2006) Beta1-adrenergic receptors maintain fetal heart rate and survival. *Biol Neonate* **89:** 147–158

Colyer J (1998) Phosphorylation states of phospholamban. *Ann NY Acad Sci* **853:** 79–91

Couette B, Marger L, Nargeot J, Mangoni ME (2006) Physiological and pharmacological insights into the role of ionic channels in cardiac pacemaker activity. *Cardiovasc Hematol Disord Drug Targets* **6:** 169–190

DiFrancesco D (1993) Pacemaker mechanisms in cardiac tissue. *Annu Rev Physiol* **55:** 455–472

DiFrancesco D, Ferroni A, Mazzanti M, Tromba C (1986) Properties of the hyperpolarizing-activated current (if) in cells isolated from the rabbit sino-atrial node. *J Physiol* **377:** 61–88

DiFrancesco D, Tortora P (1991) Direct activation of cardiac pacemaker channels by intracellular cyclic AMP. *Nature* **351:** 145–147

DiFrancesco D, Tromba C (1988) Inhibition of the hyperpolarization-activated current (i_f) induced by acetylcholine in rabbit sino-atrial node myocytes. *J Physiol* **405:** 477–491

Fabritz L, Kirchhof P, Fortmüller L, Auchampach J, Baba H, Schmitz W, Breithardt G, Neumann J, Boknik P (2004) Gene dose-dependent atrial arrhythmias, heart block and atrial brady-cardiomyopathy in mice overexpressing the A3-adenosine receptor. *Cardiovasc Res* **62:** 500–508

Gauss R, Seifert R, Kaupp UB (1998) Molecular identification of a hyperpolarization-activated channel in sea urchin sperm. *Nature* **393:** 583–587

Guo J, Ono K, Noma A (1995) A sustained inward current activated at the diastolic potential range in rabbit sino-atrial node cells. *J Physiol* **483:** 1–13

Harzheim D (2006) Der Einfluss von cAMP auf die physiologische Funktion von HCN4-Schrittmacherkanälen in der Maus. Thesis/dissertation, Universität Köln, Fatultät Math.Wat., Köln

Herrmann S, Stieber J, Stöckl G, Hofmann F, Ludwig A (2007) HCN4 provides a 'depolarization reserve' and is not required for heart rate acceleration in mice. *EMBO J* **26:** 4423–4432

Kamp TJ, Hell JW (2000) Regulation of cardiac L-type calcium channels by protein kinase A and protein kinase C. *Circ Res* **87:** 1095–1102

Kirchhof P, Fabritz L, Fortmüller L, Lankford AR, Matherne G, Baba HA, Schmitz W, Breithardt G, Neumann J, Boknik P (2003) Decreased chronotropic response to exercise and atrio-ventricular nodal conduction delay in mice overexpressing the A1-adenosine receptor. *Am J Physiol* **285:** H145–H153

Kirchhof P, Fabritz L, Zwiener M, Witt H, Schafers M, Zellerhoff S, Paul M, Athai T, Hiller KH, Baba HA, Breithardt G, Ruiz P, Wichter T, Levkau B (2006) Age- and training-dependent development of arrhythmogenic right ventricular cardiomyopathy in heterozygous plakoglobin-deficient mice. *Circulation* **114:** 1799–1806

Knollmann BC, Kirchhof P, Sirenko SG, Degen H, Greene AE, Schober T, Mackow JC, Fabritz CL, Potter JD, Morad M (2003) Familial hypertrophic cardiomyopathy-linked mutant troponin T causes stress-induced ventricular tachycardia and Ca^{2+}-dependent action potential remodeling. *Circ Res* **92:** 428–436

Kodama I, Honjo H, Boyett MR (2002) Are we lost in the labyrinth of the sinoatrial node pacemaker mechanism? *J Cardiovasc Electrophysiol* **13:** 1303–1305

Kretschmannova K, Gonzalez-Iglesias AE, Tomic M, Stojilkovic SS (2006) Dependence of hyperpolarisation-activated cyclic nucleotide-gated channel activity on basal cyclic adenosine monophosphate production in spontaneously firing GH3 cells. *J Neuroendocrinol* **18:** 484–493

Kuhlmann MT, Kirchhof P, Klocke R, Hasib L, Stypmann J, Fabritz L, Stelljes M, Tian W, Zwiener M, Mueller M, Kienast J, Breithardt G, Nikol S (2006) G-CSF/SCF reduces inducible arrhythmias in the infarcted heart potentially via increased connexin43 expression and arteriogenesis. *J Exp Med* **203:** 87–97

Lande G, Demolombe S, Bammert A, Moorman A, Charpentier F, Escande D (2001) Transgenic mice overexpressing human KvLQT1 dominant-negative isoform. Part II: Pharmacological profile. *Cardiovasc Res* **50:** 328–334

Lin W, Laitko U, Juranka PF, Morris CE (2007) Dual stretch responses of mHCN2 pacemaker channels: accelerated activation, accelerated deactivation. *Biophys J* **92:** 1559–1572

Lipsius SL, Bers DM (2003) Cardiac pacemaking: I_f versus Ca^{2+}, is it really that simple? *J Mol Cell Cardiol* **35:** 891–893

Macri V, Accili EA (2004) Structural elements of instantaneous and slow gating in hyperpolarization-activated cyclic nucleotide-gated channels. *J Biol Chem* **279:** 16832–16846

Mangoni ME, Couette B, Bourinet E, Platzer J, Reimer D, Striessnig J, Nargeot J (2003) Functional role of L-type Cav1.3 Ca^{2+} channels in cardiac pacemaker activity. *Proc Natl Acad Sci USA* **100:** 5543–5548

Mangoni ME, Traboulsie A, Leoni AL, Couette B, Marger L, Le Quang K, Kupfer E, Cohen-Solal A, Vilar J, Shin HS, Escande D, Charpentier F, Nargeot J, Lory P (2006) Bradycardia and slowing of the atrioventricular conduction in mice lacking CaV3.1/alpha1G T-type calcium channels. *Circ Res* **98:** 1422–1430

Mataruga A (2006) Licht- und elektronenmikroskopische Analyse von Bipolarzelltypen in der Mausretina. Thesis/dissertation, Universität Köln, Fatultät Math.Wat., Köln

McKay DB, Weber IT, Steitz TA (1982) Structure of catabolite gene activator protein at 2.9-Å resolution. Incorporation of amino sequence and interactions with cyclic AMP. *J Biol Chem* **257:** 9518–9524

Milanesi R, Baruscotti M, Gnecchi-Ruscone T, DiFrancesco D (2006) Familial sinus bradycardia associated with a mutation in the cardiac pacemaker channel. *N Engl J Med* **354:** 151–157

Mistrik P, Pfeifer A, Biel M (2006) The enhancement of HCN channel instantaneous current facilitated by slow deactivation is regulated by intracellular chloride concentration. *Pflügers Arch* **452:** 718–727

Pian P, Bucchi A, Robinson RB, Siegelbaum SA (2006) Regulation of gating and rundown of HCN hyperpolarization-activated channels by exogenous and endogenous PIP_2. *J Gen Physiol* **128:** 593–604

Platzer J, Engel J, Schrott-Fischer A, Stephan K, Bova S, Chen H, Zheng H, Striessnig J (2000) Congenital deafness and sinoatrial node dysfunction in mice lacking class D L-type Ca^{2+} channels. *Cell* **102:** 89–97

Portbury AL, Chandra R, Groelle M, McMillian MK, Elias A, Herlong JR, Rios M, Roffler-Tarlov S, Chikaraishi DM (2003) Catecholamines act via a beta-adrenergic receptor to maintain fetal heart rate and survival. *Am J Physiol Heart Circ Physiol* **284:** H2069–H2077

Proenza C, Yellen G (2006) Distinct populations of HCN pacemaker channels produce voltage-dependent and voltage-independent currents. *J Gen Physiol* **127:** 183–190

Rideout III WM, Wakayama T, Wutz A, Eggan K, Jackson-Grusby L, Dausman J, Yanagimachi R, Jaenisch R (2000) Generation of mice from wild-type and targeted ES cells by nuclear cloning. *Nat Genet* **24:** 109–110

Robinson RB, Brink PR, Cohen IS, Rosen MR (2006) I_f and the biological pacemaker. *Pharmacol Res* **53:** 407–415

Scholten A (2001) Charakterisierung von hyperpolarisations-aktivierten und zyklisch Nukleotid-gesteuerten Ionenkanälen (HCN-Kanäle) in der Retina und im Gehirn der Ratte. Thesis/dissertation, Universität Köln, Fatultät Math.Wat., Köln

Schulze-Bahr E, Neu A, Friedrich P, Kaupp UB, Breithardt G, Pongs O, Isbrandt D (2003) Pacemaker channel dysfunction in a patient with sinus node disease. *J Clin Invest* **111:** 1537–1545

Schwenk F, Baron U, Rajewsky K (1995) A Cre-transgenic mouse strain for the ubiquitous deletion of *loxP*-flanked gene segments including deletion in germ cells. *Nucleic Acids Res* **23:** 5080–5081

Shinagawa Y, Satoh H, Noma A (2000) The sustained inward current and inward rectifier K^+ current in pacemaker cells dissociated from rat sinoatrial node. *J Physiol* **523:** 593–605

Stieber J, Herrmann S, Feil S, Löster J, Feil R, Biel M, Hofmann F, Ludwig A (2003) The hyperpolarization-activated channel HCN4 is required for the generation of pacemaker action potentials in the embryonic heart. *Proc Natl Acad Sci USA* **100:** 15235–15240

Thomas D, Kiehn J, Katus HA, Karle CA (2003) Defective protein trafficking in hERG-associated hereditary long QT syndrome (LQT2): molecular mechanisms and restoration of intracellular protein processing. *Cardiovasc Res* **60:** 235–241

Verheijck EE, van Ginneken AC, Wilders R, Bouman LN (1999) Contribution of L-type Ca^{2+} current to electrical activity in sinoatrial nodal myocytes of rabbits. *Am J Physiol* **276:** H1064–H1077

Vinogradova TM, Lyashkov AE, Zhu W, Ruknudin AM, Sirenko S, Yang D, Deo S, Barlow M, Johnson S, Caffrey JL, Zhou YY, Xiao RP, Cheng H, Stern MD, Maltsev VA, Lakatta EG (2006) High basal protein kinase A-dependent phosphorylation drives rhythmic internal Ca^{2+} store oscillations and spontaneous beating of cardiac pacemaker cells. *Circ Res* **98:** 505–514

Wachten S, Schlenstedt J, Gauss R, Baumann A (2006) Molecular identification and functional characterization of an adenylyl cyclase from the honeybee. *J Neurochem* **96:** 1580–1590

Zagotta WN, Olivier NB, Black KD, Young EC, Olson R, Gouaux E (2003) Structural basis for modulation and agonist specificity of HCN pacemaker channels. *Nature* **425:** 200–205

Zhang Z, Xu Y, Song H, Rodriguez J, Tuteja D, Namkung Y, Shin HS, Chiamvimonvat N (2002) Functional roles of Ca(v)1.3 (alpha(1D)) calcium channel in sinoatrial nodes: insight gained using gene-targeted null mutant mice. *Circ Res* **90:** 981–987

Zolles G, Klöcker N, Wenzel D, Weisser-Thomas J, Fleischmann BK, Roeper J, Fakler B (2006) Pacemaking by HCN channels requires interaction with phosphoinositides. *Neuron* **52:** 1027–1036